

This is the accepted manuscript made available via CHORUS. The article has been published as:

$\beta$ -decay Q values among the  $A=50$  Ti-V-Cr isobaric triplet and atomic masses of  $^{46,47,49,50}\text{Ti}$ ,  $^{50,51}\text{V}$ , and  $^{50,52-54}\text{Cr}$

R. M. E. B. Kandegedara, G. Bollen, M. Eibach, N. D. Gamage, K. Gulyuz, C. Izzo, M.

Redshaw, R. Ringle, R. Sandler, and A. A. Valverde

Phys. Rev. C **96**, 044321 — Published 20 October 2017

DOI: [10.1103/PhysRevC.96.044321](https://doi.org/10.1103/PhysRevC.96.044321)

# $\beta$ -decay $Q$ values among the $A = 50$ Ti-V-Cr isobaric triplet and atomic masses of $^{46,47,49,50}\text{Ti}$ , $^{50,51}\text{V}$ , and $^{50,52-54}\text{Cr}$

R.M.E.B. Kandegedara,<sup>1</sup> G. Bollen,<sup>2,3</sup> M. Eibach,<sup>4,5</sup> N.D. Gamage,<sup>1,6</sup> K. Gulyuz,<sup>4</sup>  
C. Izzo,<sup>3,4</sup> M. Redshaw,<sup>1,4,6,\*</sup> R. Ringle,<sup>4</sup> R. Sandler,<sup>1,3,4,6</sup> and A.A. Valverde<sup>3,4,†</sup>

<sup>1</sup>*Department of Physics, Central Michigan University, Mount Pleasant, Michigan 48859, USA*

<sup>2</sup>*Facility for Rare Isotope Beams, East Lansing, Michigan 48824, USA*

<sup>3</sup>*Department of Physics and Astronomy, Michigan State University, East Lansing, Michigan 48824, USA*

<sup>4</sup>*National Superconducting Cyclotron Laboratory, East Lansing, Michigan 48824 USA*

<sup>5</sup>*Universität Greifswald, 17487 Greifswald, Germany*

<sup>6</sup>*Science of Advanced Materials Program, Central Michigan University, Mount Pleasant, Michigan 48859, USA*

Using high-precision Penning trap mass spectrometry at the LEBIT facility we have measured the  $Q$  values of the 4th order forbidden  $\beta$ -decay and electron capture of  $^{50}\text{V}$  and the double electron capture  $Q$  value of  $^{50}\text{Cr}$  with the results  $Q_{\beta}(^{50}\text{V}) = 1038.1(1)$  keV,  $Q_{EC}(^{50}\text{V}) = 2208.7(1)$  keV,  $Q_{2EC}(^{50}\text{Cr}) = 1170.5(1)$  keV. In addition, we have measured the atomic masses of  $^{46,47,49,50}\text{Ti}$ ,  $^{50,51}\text{V}$ , and  $^{50,52-54}\text{Cr}$ , reducing uncertainties by factors of up to 3 compared to the most recent atomic mass evaluation (AME2016) [M. Wang, *et.al.*, Chin. Phys. **41**, 030003 (2017)]. Our results are in good agreement with AME2016 for  $^{46,47,49,50}\text{Ti}$  and  $^{50,54}\text{Cr}$ , and show deviations of up to  $\sim 1$  keV ( $2.5\sigma$ ) for  $^{50,51}\text{V}$  and  $^{50,54}\text{Cr}$ .

PACS numbers: 23.40.-s, 32.10.Bi, 27.60.+j, 07.75.+h

## I. INTRODUCTION

In nature, only three nuclei are known to exist for which the dominant decay process is a four-fold forbidden non-unique  $\beta$ -decay.  $^{50}\text{V}$  stands alone among the three in that it can undergo electron capture (EC)—to the  $2^+$  state in  $^{50}\text{Ti}$ , or  $\beta$ -decay—to the  $2^+$  state in  $^{50}\text{Cr}$  (see the decay scheme in Fig. 1). The other two,  $^{113}\text{Cd}$  and  $^{115}\text{In}$ , both undergo  $\beta$ -decay to the ground states of their respective daughter nuclides. The fact that  $^{50}\text{Cr}$  is more strongly bound than  $^{50}\text{V}$ , but less so than  $^{50}\text{Ti}$ , means that  $^{50}\text{Cr}$  is unstable against double electron capture (2EC) to the  $^{50}\text{Ti}$  ground state. Experimental searches for all three decays in this isobaric triplet have been undertaken e.g. most recently [1, 2].

The electron capture decay of  $^{50}\text{V}$  to  $^{50}\text{Ti}(2^+)$  was first observed in 1984 by Alburger *et. al.* [3] and in further experiments in the 1980s by Simpson *et. al.* [4, 5]. The half-life was measured recently and more precisely using modern low background techniques, with the result  $T_{1/2}^{EC} = (2.29 \pm 0.25) \times 10^{17}$  yr [1]. Attempts to observe  $^{50}\text{V}$   $\beta$ -decay to  $^{50}\text{Cr}(2^+)$  have produced only lower limits on the half-life for this decay branch, except for one claimed observation [5]. However, this result was not confirmed by the recent experiment of Ref. [1], which saw no indication of this decay branch and provided a lower limit  $T_{1/2}^{\beta} > 1.5 \times 10^{18}$  yr. Recent theoretical descriptions of  $^{50}\text{V}$  electron capture and  $\beta$ -decay have provided calculated half-lives of  $\approx 4 \times 10^{17}$  yr and  $\approx 2 \times 10^{19}$  yr for the electron capture and  $\beta$ -decay modes respectively [6]. The

calculated electron capture half-life is in good agreement with the experimental observations and the calculated  $\beta$ -decay half-life indicates that this decay could be observed in an experiment with existing low background facilities and an achievable increase in source material.

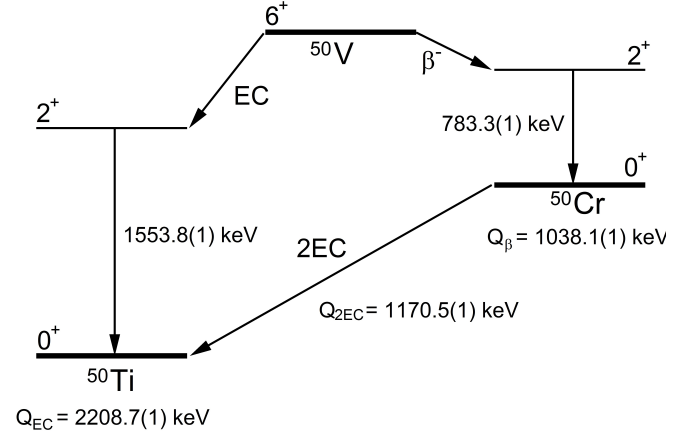


FIG. 1. Nuclear level scheme for  $\beta$ -decay and electron-capture decay of  $^{50}\text{V}$  and double electron capture decay of  $^{50}\text{Cr}$ . The  $Q$  values are the ground-state to ground-state transition  $Q$  values i.e. the energy equivalent of the mass difference between parent and daughter atoms.

In this paper, we report on the first direct determination of the  $Q$  values  $Q_{EC}(^{50}\text{V} \rightarrow ^{50}\text{Ti})$ ,  $Q_{\beta}(^{50}\text{V} \rightarrow ^{50}\text{Cr})$ , and  $Q_{2EC}(^{50}\text{Cr} \rightarrow ^{50}\text{Ti})$  using high-precision Penning trap mass spectrometry. These data provide precise inputs for determinations of the phase space factors that appear in the theoretical descriptions of the decays to determine the partial half-lives. In the case of  $\beta$ -decay the phase space factor appears in the calculation of the spectral shape, which is of interest for comparing theoretical pre-

\* redsh1m@cmich.edu

† Current address: Department of Physics, University of Notre Dame, Notre Dame, Indiana, 46556, USA

dictions with experimental results [7] and as a possible method for extracting information on the magnitude of the axial vector coupling constant,  $g_A$  [8–10]. The  $Q$  value also defines the end-point of the  $\beta$ -decay energy spectrum, which provides a strong test of systematics for detectors used to observe these decays, e.g. as was done in the case of  $^{113}\text{Cd}$  [11]. In addition we report improved values for the atomic masses of  $^{46,47,49,50}\text{Ti}$ ,  $^{50,51}\text{V}$ , and  $^{50,52-54}\text{Cr}$ . These results are important for testing the reliability of input data used in global evaluations of atomic masses i.e. the atomic mass evaluation [12], and improving its overall accuracy.

## II. EXPERIMENTAL METHOD

The Low Energy Beam and Ion Trap (LEBIT) facility located at the National Superconducting Cyclotron Laboratory (NSCL) was used to perform  $Q$  value and absolute atomic mass determinations by measuring the cyclotron frequencies of singly-charged titanium, vanadium and chromium ions in a Penning trap. The LEBIT facility was designed for online mass measurements of rare isotopes produced at the NSCL [13]. However, offline sources, including a plasma source and a recently commissioned laser ablation source (LAS) [14] enable access to a wide range of stable and long-lived isotopes. Ions from these sources are used for calibration purposes and for mass and  $Q$  value determinations with applications, for example, in nuclear and neutrino physics [11, 15–20]. A schematic diagram of the sections of the LEBIT facility used in this work is shown in Fig. 2.

The LAS employs a frequency doubled pulsed Nd:YAG laser that can deliver up to 160 mJ per 4 ns pulse. The laser beam is focused onto an ablation target with a sub-mm spot size to produce power densities of up to  $\sim 10^8$  W/cm<sup>2</sup>. In this measurement campaign, high purity titanium, vanadium and chromium foils, typically 0.5 – 1 mm thick, with natural isotopic abundances were installed in the LAS. As such, ions of all naturally occurring isotopes of these elements could be produced:  $^{46-50}\text{Ti}$ ,  $^{50,51}\text{V}$ ,

$^{50,52-54}\text{Cr}$ . Of these isotopes  $^{50}\text{V}$  has the lowest natural abundance (0.25%). Nevertheless, it was possible to produce sufficient quantities of  $^{50}\text{V}^+$  ions and remove  $^{51}\text{V}^+$  and any other contaminants from the beam and trap, as described below.

After the laser pulse is incident on the target material, ablated ions are extracted from the surface of the target and accelerated to 5 keV. Ions are then bent through 90° by a quadrupole bender and directed into a beam cooler and buncher [21, 22]. In the cooler/buncher ions are thermalized via their interaction with a low pressure helium buffer gas inside a linear radio frequency (RF) quadrupole trap. Thermalized ions are accumulated in an axial potential-well superimposed over the RF trapping field before being ejected as a low-emittance,  $\sim 100$  ns duration ion bunch. Ions are then accelerated to 2 keV and transported toward the Penning trap. Before entering the fringe field of the magnet the ions pass through a fast-switching electrostatic gate which allows through ions of a single  $A/q$  while any other ions in the beam are rejected. After they enter the magnetic field, ions are decelerated by a series of retarding electrodes before being captured in the Penning trap. The final retardation electrode is radially four-way segmented to create a “Lorentz” steerer, enabling precise control over the ion’s initial radial amplitude and phase in the Penning trap [23].

The LEBIT Penning trap consists of an eight-fold segmented hyperbolic ring electrode, two hyperbolic end-cap electrodes, and two correction ring and correction tube electrodes [24], and is housed inside a 9.4 T superconducting solenoidal magnet. The electrodes produce a quadratic electrostatic potential that confines the ions axially, along the direction of the magnetic field. Radial confinement is provided by the magnetic field that, in the absence of the electric field, causes the ions to undergo cyclotron motion at the free-space cyclotron frequency

$$f_c = \frac{1}{2\pi} \frac{qB}{m}. \quad (1)$$

The addition of the electric field results in three normal modes of motion for an ion in the Penning trap: the trap-cyclotron, magnetron, and axial modes, with frequencies  $f_+$ ,  $f_-$ , and  $f_z$ , respectively. The free-space cyclotron frequency and the radial normal mode frequencies are related via [25, 26]

$$f_c = f_+ + f_-. \quad (2)$$

For more details on Penning trap physics see, for example, the review articles of Ref. [27, 28].

After ions are captured in the Penning trap, contaminant ions are removed from the trap by applying a pulsed RF dipole drive at their trap-cyclotron frequency. The time-of-flight ion cyclotron resonance (TOF-ICR) technique [29] is then used to measure the cyclotron frequency of the ion of interest. This technique is well documented in the literature, so is only briefly reviewed here.

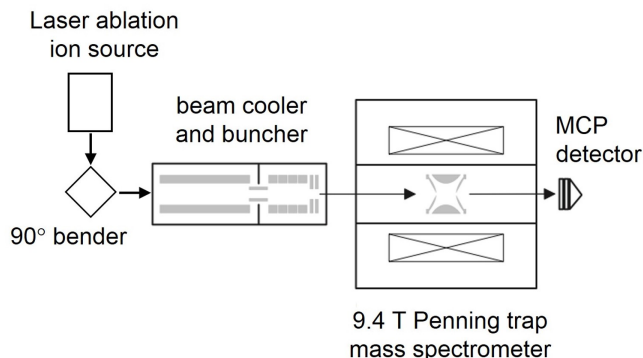


FIG. 2. Schematic diagram showing the subset of components of the LEBIT facility used in this work.

A quadrupole rf drive at the frequency  $f_{\text{rf}}$  close to the sum frequency  $f_+ + f_-$  is applied to ions in the Penning trap, which couples their magnetron and cyclotron modes. The drive amplitude and duration are chosen such that, when the correct frequency is applied, a full conversion is made of the ions' initial magnetron motion into cyclotron motion. Next the ions are ejected from the trap toward a microchannel plate detector (MCP) located in the fringe field of the magnet. Due to the interaction of the ions' magnetic moment with the magnetic field gradient, the time-of-flight to the MCP depends on the ions' cyclotron amplitude in the trap. Hence, when  $f_{\text{rf}} = f_+ + f_-$ , the cyclotron amplitude is maximized and the time-of-flight is minimized. To determine the optimal value of  $f_{\text{rf}}$  that minimizes the time-of-flight, a series of measurements are performed on sequentially trapped ions bunches in which  $f_{\text{rf}}$  is systematically varied, and a TOF resonance curve such as the one shown in Fig. 3 (a) is obtained. A fit of the theoretical line shape [30] to this curve is then used to extract the value of  $f_{\text{rf}}$  for the minimum time-of-flight that, according to Eqn. 2, corresponds to the free-space cyclotron frequency.

For the data used in our final analysis, a Ramsey quadrupole excitation scheme was used to couple the magnetron and cyclotron modes [31, 32]. This scheme modifies the TOF curve to that of Fig. 3 (b), which is again fit with the theoretical line shape [33]. This technique results in a narrower central peak in the TOF curve compared to the traditional TOF-ICR technique, and a factor of  $\sim 3$  increase in precision in  $f_c$  for the same measurement time.

In order to calibrate the magnetic field and to account for its time variation, cyclotron frequency measurements on the ion of interest,  $f_c^{\text{ion}}$ , and a reference ion,  $f_c^{\text{ref}}$ , are alternately performed. Typically, two reference ion measurements at times  $t_0$  and  $t_2$  encompass each measurement of the ion of interest at time  $t_1$ . The frequencies of the reference ion measurements are interpolated to obtain  $f_c^{\text{ref}}$  at time  $t_1$ . The cyclotron frequency ratio, which corresponds to the inverse mass ratio of the ions, is hence obtained:

$$R = \frac{f_c^{\text{ref}}(t_1)}{f_c^{\text{ion}}(t_1)} = \frac{m_{\text{ion}} - m_e + b_{\text{ion}}/c^2}{m_{\text{ref}} - m_e + b_{\text{ref}}/c^2}. \quad (3)$$

Here,  $m_{\text{ref}}$  and  $m_{\text{ion}}$  are the neutral atomic masses of the reference and nuclide of interest, respectively,  $b_{\text{ref}}$  and  $b_{\text{ion}}$  are (in this case for singly charged atoms) their first ionization energies,  $m_e$  is the mass of the electron, and  $c$  is the speed of light. The cyclotron frequency ratio is obtained for all such alternating pairs of cyclotron frequency measurements and the average ratio,  $\bar{R}$ , for the data set is obtained as a weighted average.

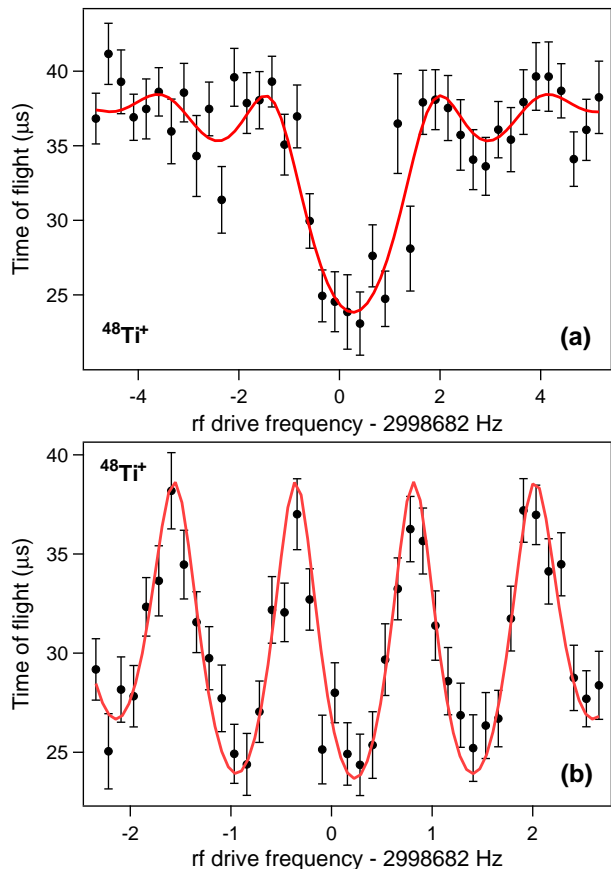


FIG. 3. (Color online) Time-of-flight ion cyclotron frequency resonances for  $^{48}\text{Ti}^+$  using (a) a 0.5 s traditional quadrupole excitation scheme, and (b) a 1.0 s Ramsey quadrupole excitation scheme. The solid lines are fits of the theoretical line shapes to the data for the traditional [30] or Ramsey [33] schemes.

### III. DATA AND ANALYSIS

In this work a 200-600-200 ms rf on-off-on two-pulse Ramsey scheme was used. A frequency range of  $\pm 2.5$  Hz around the resonant frequency was scanned in 125 mHz steps and typically 1 – 2 ions were detected per shot, producing a Ramsey TOF resonance, such as the one shown in Fig. 3 (b). When the detected ion number was greater than 5, these data were removed from the analysis to eliminate possible systematic frequency shifts due to the Coulomb interaction between ions in the trap [34–36]. The scan over the entire frequency range was repeated 30 times to accumulate statistics. As such, each resonance took about 30 mins to acquire and typically contained around 2000 detected ions.

For each ion pair for which the cyclotron frequency ratio was measured, between 9 and 33 individual ratio measurements were obtained using Eqn. 3 and the average ratio was found. Fig. 4 shows an example of cyclotron frequency ratio data for  $^{50}\text{V}^+ / ^{50}\text{Cr}^+$ . For each of these data sets, the Birge ratio [37] was calculated. In cases

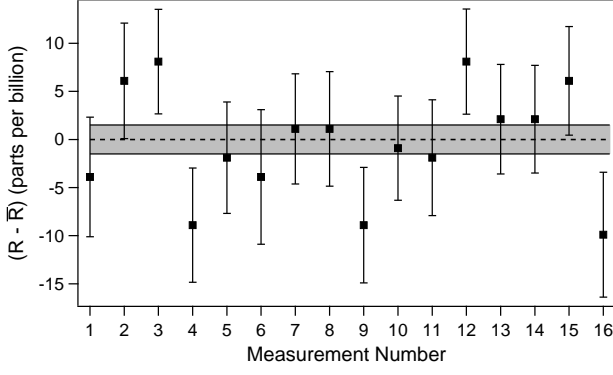


FIG. 4. Individual cyclotron frequency ratio measurements,  $R$ , of  $^{50}\text{V}^+ / ^{50}\text{Cr}^+$ , each obtained from pairs of frequency measurements similar to that of Fig. 3 (b), and calculated using Eqn. 3. The dotted line and shaded region indicate the weighted average and corresponding uncertainty, as listed in Table I.

where the Birge ratio,  $BR$ , was greater than 1, the statistical uncertainty in  $\bar{R}$  was inflated by the factor  $BR$ . The resulting ratios are listed in Table I.

The main goal of this work was to measure the  $^{50}\text{V}$   $Q_{EC}$  and  $Q_\beta$  values, and the  $^{50}\text{Cr}$   $Q_{2EC}$  value. These quantities are defined as the energy equivalent of the mass difference between relevant parent and daughter atoms, via:

$$Q = [m_p - m_d] c^2, \quad (4)$$

where  $m_p$  and  $m_d$  are the mass of the parent and daughter atoms, respectively. Atomic masses can be obtained from Eqn. 3, which can be arranged in the form of a

TABLE I. Average cyclotron frequency ratios,  $\bar{R}$ , for the ion pairs listed with statistical uncertainties in parentheses.  $N$  is the number of measurements used to determine the average for each ion pair,  $BR$  is the Birge ratio.

Num	Ion Pair	$N$	$BR$	$\bar{R}$
(1)	$^{50}\text{V}^+ / ^{50}\text{Ti}^+$	11	0.79	0.999 952 526 6(23)
(2)	$^{50}\text{V}^+ / ^{50}\text{Cr}^+$	16	0.98	0.999 977 687 9(15)
(3)	$^{48}\text{Ti}^+ / ^{46}\text{Ti}^+$	21	0.95	0.958 385 341 6(13)
(4)	$^{48}\text{Ti}^+ / ^{47}\text{Ti}^+$	21	0.97	0.979 223 413 2(12)
(5)	$^{48}\text{Ti}^+ / ^{49}\text{Ti}^+$	21	0.83	1.020 854 600 8(11)
(6)	$^{48}\text{Ti}^+ / ^{50}\text{Ti}^+$	33	0.85	1.041 646 581 7(10)
(7)	$^{48}\text{Ti}^+ / ^{50}\text{V}^+$	12	0.87	1.041 696 034 7(23)
(8)	$^{48}\text{Ti}^+ / ^{51}\text{V}^+$	16	1.08	1.062 485 504 2(17)
(9)	$^{48}\text{Ti}^+ / ^{50}\text{Cr}^+$	11	0.75	1.041 672 787 6(15)
(10)	$^{48}\text{Ti}^+ / ^{52}\text{Cr}^+$	10	1.03	1.083 269 683 4(20)
(11)	$^{48}\text{Ti}^+ / ^{53}\text{Cr}^+$	9	0.97	1.104 128 820 5(24)
(12)	$^{48}\text{Ti}^+ / ^{54}\text{Cr}^+$	9	1.37	1.124 948 122 4(33)

mass difference equation

$$m_{\text{ref}} - m_{\text{ion}} = [m_{\text{ref}} - m_e] (1 - \bar{R}) + \frac{b_{\text{ion}}}{c^2} - \frac{b_{\text{ref}}}{c^2} \bar{R}. \quad (5)$$

Hence, the  $Q$  value can be indirectly determined from two ratio measurements that are used to determine the atomic masses of parent and daughter atoms respectively. Alternatively, if the reference ion and ion of interest are chosen to be ions of the parent and daughter atoms, respectively, the  $Q$  value can be obtained directly from a single ratio measurement:

$$Q = [(m_p - m_e) c^2 + b_p] (1 - \bar{R}) + b_d - b_p, \quad (6)$$

where the subscripts p and d refer to the parent and daughter atoms, respectively. In this work, singly-charged titanium, chromium and vanadium ions were used. The corresponding first ionization energies are:  $b_{\text{Ti}} = 6.83$  eV,  $b_{\text{Cr}} = 6.77$  eV,  $b_{\text{V}} = 6.75$  eV [38]. We note that the uncertainties in these ionization energies (all <10 meV), and any differences among the different isotopes of each element are insignificant at the level of precision of this work.

## IV. RESULTS AND DISCUSSION

### A. $Q$ values among $^{50}\text{Ti}$ , $^{50}\text{V}$ , and $^{50}\text{Cr}$

The  $^{50}\text{V}$   $Q_{EC}$  and  $Q_\beta$  values were obtained with Eqn. 6 using ratios (1) and (2) listed in Table I. The mass of the parent atom, in this case  $^{50}\text{V}$ , does appear in the right hand side of Eqn. 6. For this calculation we used the new value for  $m(^{50}\text{V})$  obtained in this work—see section IV. B.—and the conversion factor 931 494.0954(57) keV/ $c^2$  per u [39] to obtain the  $Q$  value in keV. However, we note that the sensitivity of the calculated  $Q$  value to the uncertainty in the mass of the parent atom is reduced by a factor  $(1 - \bar{R}) < 10^{-4}$ , which is completely negligible at our level of precision. We also obtained the  $^{50}\text{V} \rightarrow ^{50}\text{Cr}$   $\beta$ -decay  $Q$  value indirectly from Eqn. 4, using ratios (7) and (9) and Eqn. 5 to determine the mass of  $^{50}\text{V}$ , and  $^{50}\text{Cr}$ , respectively. Ratios (7) and (9) use the same reference ion,  $^{48}\text{Ti}^+$ , so the uncertainty in the reference ion mass drops out in the  $Q$  value determination. The  $Q$  value obtained from these two independent determinations agreed at the  $1.5\sigma$  level. To account for the possible discrepancy between the two measurements we followed the procedure of the Particle Data Group [40] and inflated the uncertainty in the average by the factor 1.5, which corresponds to the scale factor defined in Ref. [40].

Finally, we obtained the  $^{50}\text{Cr}$   $Q_{2EC}$  value indirectly in two ways—by determining the  $^{50}\text{Cr}$  and  $^{50}\text{Ti}$  masses from ratios (1) and (2), using  $^{50}\text{V}$  as a reference, and by determining the  $^{50}\text{Cr}$  and  $^{50}\text{Ti}$  masses from ratios (6) and (9), using  $^{48}\text{Ti}$  as a reference (again, then uncertainty due to the reference ions drops out). Here, the  $Q$  value

TABLE II.  $Q$  values (in keV) for the  $\beta$ -decay and EC decay of  $^{50}\text{V}$  and the 2EC decay of  $^{50}\text{Cr}$  obtained from the cyclotron frequency ratios listed in Table I.

Decay	Ref	Q value (keV)		$\Delta Q$ (keV/ $c^2$ )
		This work	AME2016	
$^{50}\text{V}(\text{EC})$	direct	2208.70(11)	2207.65(43)	1.05(44)
$^{50}\text{V}(\beta^-)$	direct	1038.07(7)		
	$^{48}\text{Ti}$	1038.28(12)		
	avg	1038.12(9)	1038.06(59)	0.06(60)
	$^{50}\text{V}$	1170.63(13)		
$^{50}\text{Cr}(\text{2EC})$	$^{48}\text{Ti}$	1170.43(8)		
	avg	1170.48(10)	1169.59(45)	0.90(46)

obtained from the two methods agreed at the  $1.4\sigma$  level and so we inflated the uncertainty in the average by 1.4.

The resulting  $Q$  values obtained from the different methods, the average values, and a comparison with values from the 2016 Atomic Mass Evaluation (AME2016) [12] are listed in Table II. We find that our result for the  $^{50}\text{V}$   $Q_\beta$  value is in good agreement with the AME2016 data, whereas our  $^{50}\text{V}$   $Q_{\text{EC}}$  and  $^{50}\text{Cr}$   $Q_{\text{2EC}}$  measurements show a  $2\sigma$  shift of around 1 keV compared to the AME2016. As discussed in section IV. B., this shift is due to the fact that our values for the atomic masses of  $^{50}\text{V}$  and  $^{50}\text{Cr}$  are shifted from the AME2016 values by about 1 keV.

### B. Atomic mass determinations for $^{46,47,49,50}\text{Ti}$ , $^{50,51}\text{V}$ , and $^{50,52-54}\text{Cr}$

The absolute masses of  $^{46,47,49,50}\text{Ti}$ ,  $^{50,51}\text{V}$ , and  $^{50,52-54}\text{Cr}$  were determined from the cyclotron frequency ratio measurements (3) – (12) in Table I and using Eqn. 5. In each case  $^{48}\text{Ti}^+$  was the reference ion and the value  $m(^{48}\text{Ti}) = 47.947\,940\,932(117)$  u given in the AME2016 [12] was used. This value is mainly determined from precise Penning trap measurements of the atomic mass of  $^{48}\text{Ca}$  [15] and of the  $^{48}\text{Ca}$ – $^{48}\text{Ti}$  double  $\beta$ -decay  $Q$  value [16, 41]. A recent Penning trap determination of the mass of  $^{48}\text{Ca}$  [42], not included in the AME2016, reduces its uncertainty by a factor of  $\sim 10$ , but is in agreement with the result of Ref. [15].

Our resulting atomic masses were converted into mass excesses and are listed in Table III. The difference between our results and the AME2016 values are also listed in Table III and are plotted in Figure 5.

#### 1. Atomic masses of $^{46,47,49,50}\text{Ti}$

Our results for the atomic masses of  $^{47,49,50}\text{Ti}$  are in excellent agreement with the values listed in AME2016. These values are either completely or mainly determined

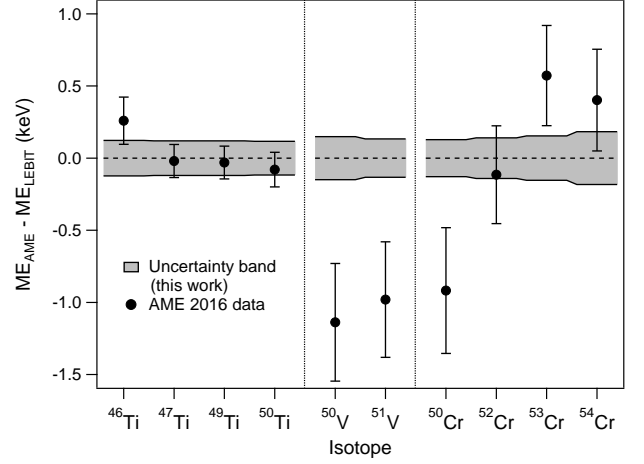


FIG. 5. Difference between mass excesses given in the AME2016 and those determined in this work. The shaded band corresponds to the total uncertainty in our mass measurements, as listed in the second column of Table III.

from  $(n,\gamma)$  reactions i.e. neutron binding energy measurements, performed via  $\gamma$ -ray spectroscopy after neutron capture on  $^{47,48,49}\text{Ti}$ , that link them to the mass of  $^{48}\text{Ti}$ . Our value for the mass of  $^{46}\text{Ti}$  is also in good agreement with the AME2016 value, which was determined via  $(p,\gamma)$ ,  $(^3\text{He},t)$ , and  $(d,p)$  reactions. Due to the uncertainty in the mass of  $^{48}\text{Ti}$  of 0.11 keV, our new results do not reduce the uncertainties in the masses of  $^{47,49,50}\text{Ti}$ , but reduce the  $^{46}\text{Ti}$  uncertainty by a factor of 1.3 compared to the AME2016.

TABLE III. Mass excesses, ME, for  $^{46,47,49,50}\text{Ti}$ ,  $^{50,51}\text{V}$ , and  $^{50,52-54}\text{Cr}$  obtained from the cyclotron frequency ratios listed in Table I, and mass differences,  $\Delta M$ , between the AME2016 [12] values and our new results. The uncertainties given in parentheses in the second column correspond to the statistical uncertainty, uncertainty in the reference ( $^{48}\text{Ti}$ ), and total uncertainty, respectively.

Isotope	ME (keV/ $c^2$ )		$\Delta M$ (keV/ $c^2$ )
	This work	AME2016	
$^{46}\text{Ti}$	-44 128.06(6)(11)(12)	-44 127.80(16)	0.26(21)
$^{47}\text{Ti}$	-44 937.35(5)(11)(12)	-44 937.37(11)	-0.02(17)
$^{49}\text{Ti}$	-48 563.76(5)(11)(12)	-48 563.79(11)	-0.03(17)
$^{50}\text{Ti}$	-51 431.58(4)(11)(12)	-51 431.66(12)	-0.08(17)
$^{50}\text{V}$	-49 222.88(10)(11)(15)	-49 224.02(41)	-1.14(43)
$^{51}\text{V}$	-52 202.87(8)(11)(13)	-52 203.85(40)	-0.98(42)
$^{50}\text{Cr}$	-50 261.16(7)(11)(13)	-50 262.08(44)	-0.92(45)
$^{52}\text{Cr}$	-55 419.13(9)(11)(14)	-55 419.25(34)	-0.11(37)
$^{53}\text{Cr}$	-55 287.58(11)(11)(15)	-55 287.01(35)	0.57(38)
$^{54}\text{Cr}$	-56 935.17(15)(11)(18)	-56 934.77(35)	0.40(40)

TABLE IV. Neutron separation energies obtained via cyclotron frequency ratio measurements described here,  $E_n$ , and from  $\gamma$ -ray spectroscopy measurements performed after neutron capture on  $^{47,48,49}\text{Ti}$ ,  $E_\gamma$  [43, 44].

Isotope	$E_n$ (keV)	$E_\gamma$ (keV)	$E_\gamma - E_n$ (keV)
$^{48}\text{Ti}$	11 626.68(5)	11 626.65(4)	-0.03(7)
$^{49}\text{Ti}$	8 142.37(5)	8 142.39(3)	0.02(6)
$^{50}\text{Ti}$	10 939.14(7)	10 939.19(3)	0.05(7)

### 2. Neutron separation energies of $^{48,49,50}\text{Ti}$

From our cyclotron frequency ratio measurements of  $^{48}\text{Ti}^+ / ^{47}\text{Ti}^+$ ,  $^{48}\text{Ti}^+ / ^{49}\text{Ti}^+$ , and  $^{48}\text{Ti}^+ / ^{50}\text{Ti}^+$ , and using Eqn. 5, we can obtain the mass difference,  $\Delta m$ , between  $^{47}\text{Ti}$ - $^{48}\text{Ti}$ ,  $^{48}\text{Ti}$ - $^{49}\text{Ti}$ , and  $^{49}\text{Ti}$ - $^{50}\text{Ti}$ . Hence, we can determine the neutron separation energy  $E_n = m_n - \Delta m$ , where  $m_n$  is the mass of the neutron. These results can be directly compared with the  $(n, \gamma)$  measurements of Ref. [43, 44] that are used in the AME2016 evaluation, see Table IV. This comparison provides a test of  $E = mc^2$ , similar to that described in Ref. [45], but is a factor of about 10 less precise. However, improvements in the precision of the mass measurements are possible with existing or upcoming facilities e.g. [46, 47] and the  $\gamma$ -ray spectroscopy measurement could be performed more precisely using the GAMS4 crystal diffraction spectrometer [48].

### 3. Atomic masses of $^{50,51}\text{V}$

Our new results for the mass of  $^{50,51}\text{V}$  indicate a shift of about 1 keV with respect to the AME2016 and an increase in precision of a factor of 3 in both cases. The mass of  $^{50}\text{V}$  is determined from nuclear reaction data, whereas the mass of  $^{51}\text{V}$  was determined from a Penning trap measurement [49] and from  $(p, n)$  reaction data, linking it to  $^{51}\text{Cr}$  [50]. The  $^{51}\text{Cr}$  mass was also determined in the Penning trap measurement of Ref. [49]. Our value for  $m(^{51}\text{V})$  and that of Ref. [49] differ by 0.82(55) keV, i.e.  $1.5\sigma$ .

### 4. Atomic masses of $^{50,52-54}\text{Cr}$

For the chromium masses, our results indicate that the AME2016 value for  $^{50}\text{Cr}$  is too low by about 1 keV, a

$2\sigma$  difference. The value for  $^{54}\text{Cr}$  is too large by 0.6 keV ( $1.5\sigma$ ) and the values for  $^{52,53}\text{Cr}$  agree at the  $1\sigma$  level or better. In each case we improve the uncertainties by factors of  $\sim 2-3$ . Only  $^{52}\text{Cr}$  was previously determined via a direct Penning trap measurement. This measurement was performed with the ISOLTRAP facility and was included in AME2016, but is currently unpublished [51]. Neutron capture  $(n, \gamma)$  measurements link the  $^{53,54}\text{Cr}$  masses to  $^{52}\text{Cr}$ , and the  $^{50}\text{Cr}$  mass to  $^{51}\text{Cr}$ .

## V. CONCLUSION

We have performed the first direct measurement of the  $^{50}\text{V}$   $\beta$ -decay and electron capture  $Q$  values and have also provided a new determination of the  $^{50}\text{Cr}$  double electron capture  $Q$  value using high-precision Penning trap mass spectrometry. These results provide precise input data for theoretical calculations of these processes and can be used to help analyze experimental data. We also report on the first measurements of the masses of  $^{46,47,49,50}\text{Ti}$ ,  $^{50}\text{V}$ , and  $^{50,53,54}\text{Cr}$  via Penning trap mass spectrometry, and provide more precise mass values for  $^{51}\text{V}$ , and  $^{52}\text{Cr}$ , which have been previously measured with Penning traps.

## VI. ACKNOWLEDGMENTS

This research was supported by Michigan State University and the Facility for Rare Isotope Beams, the National Science Foundation under Contract No. PHY-1102511 and No. PHY-1307233, and the Central Michigan University Faculty Research and Creative Endeavors grant program. This material is based upon work supported by the U.S. Department of Energy, Office of Science, Office of Nuclear Physics under award number DE-SC0015927. The work leading to this publication has also been supported by a DAAD P.R.I.M.E. fellowship with funding from the German Federal Ministry of Education and Research and the People Programme (Marie Curie Actions) of the European Union's Seventh Framework Programme (FP7/2007/2013) under REA grant agreement no. 605728.

- 
- [1] H. Dombrowski, S. Neumaier, and K. Zuber, Phys. Rev. C **83**, 054322 (2011).
  - [2] I. Bikit, N. Zikić-Todorović, J. Slivka, M. Vesković, M. Krmar, L. Čonkić, J. Puzović, and I. V. Aničin, Phys.

Rev. C **67**, 065801 (2003).

- [3] D. E. Alburger, E. K. Warburton, and J. B. Cumming, Phys. Rev. C **29**, 2294 (1984).



- [4] J. J. Simpson, P. Jagam, and A. A. Pilt, *Phys. Rev. C* **31**, 575 (1985).
- [5] J. J. Simpson, P. Moorhouse, and P. Jagam, *Phys. Rev. C* **39**, 2367 (1989).
- [6] M. Haaranen, P. C. Srivastava, J. Suhonen, and K. Zuber, *Phys. Rev. C* **90**, 044314 (2014).
- [7] F. Quarati, P. Dorenbos, and X. Mougeot, *Applied Radiation and Isotopes* **108**, 30 (2016).
- [8] M. Haaranen, P. C. Srivastava, and J. Suhonen, *Phys. Rev. C* **93**, 034308 (2016).
- [9] M. Haaranen, J. Kotila, and J. Suhonen, *Phys. Rev. C* **95**, 024327 (2017).
- [10] J. Kostensalo, M. Haaranen, and J. Suhonen, *Phys. Rev. C* **95**, 044313 (2017).
- [11] N. D. Gamage, G. Bollen, M. Eibach, K. Gulyuz, C. Izzo, R. M. E. B. Kandegedara, M. Redshaw, R. Ringle, R. Sandler, and A. A. Valverde, *Phys. Rev. C* **94**, 025505 (2016).
- [12] M. Wang, G. Audi, F. Kondev, W. Huang, S. Naimi, and X. Xu, *Chinese Physics C* **41**, 030003 (2017).
- [13] R. Ringle, G. Bollen, and S. Schwarz, *Int. J. Mass Spectrom.* **349–350**, 87 (2013).
- [14] C. Izzo, G. Bollen, S. Bustabad, M. Eibach, K. Gulyuz, D. J. Morrissey, M. Redshaw, R. Ringle, R. Sandler, S. Schwarz, and A. A. Valverde, *Nucl. Instrum. Meth. B* **376**, 60 (2015).
- [15] M. Redshaw, G. Bollen, M. Brodeur, S. Bustabad, D. L. Lincoln, S. J. Novario, R. Ringle, and S. Schwarz, *Phys. Rev. C* **86**, 041306 (2012).
- [16] S. Bustabad, G. Bollen, M. Brodeur, D. L. Lincoln, S. J. Novario, M. Redshaw, R. Ringle, S. Schwarz, and A. A. Valverde, *Phys. Rev. C* **88**, 022501 (2013).
- [17] S. Bustabad, G. Bollen, M. Brodeur, D. L. Lincoln, S. J. Novario, M. Redshaw, R. Ringle, and S. Schwarz, *Phys. Rev. C* **88**, 035502 (2013).
- [18] D. L. Lincoln, J. D. Holt, G. Bollen, M. Brodeur, S. Bustabad, J. Engel, S. J. Novario, M. Redshaw, R. Ringle, and S. Schwarz, *Phys. Rev. Lett.* **110**, 012501 (2013).
- [19] K. Gulyuz, J. Ariche, G. Bollen, S. Bustabad, M. Eibach, C. Izzo, S. J. Novario, M. Redshaw, R. Ringle, R. Sandler, S. Schwarz, and A. A. Valverde, *Phys. Rev. C* **91**, 055501 (2015).
- [20] M. Eibach, G. Bollen, K. Gulyuz, C. Izzo, M. Redshaw, R. Ringle, R. Sandler, and A. A. Valverde, *Phys. Rev. C* **94**, 015502 (2016).
- [21] S. Schwarz, G. Bollen, D. Lawton, A. Neudert, R. Ringle, P. Schury, and T. Sun, *Nucl. Instrum. Meth. B* **204**, 474 (2003).
- [22] S. Schwarz, G. Bollen, R. Ringle, J. Savory, and P. Schury, *Nucl. Instrum. Meth. A* **816**, 131 (2016).
- [23] R. Ringle, G. Bollen, A. Prinke, J. Savory, P. Schury, S. Schwarz, and T. Sun, *International Journal of Mass Spectrometry* **263**, 38 (2007).
- [24] R. Ringle, G. Bollen, A. Prinke, J. Savory, P. Schury, S. Schwarz, and T. Sun, *Nucl. Instrum. Meth. A* **604**, 536 (2009).
- [25] G. Gabrielse, *Phys. Rev. Lett.* **102**, 172501 (2009).
- [26] G. Gabrielse, *International Journal of Mass Spectrometry* **279**, 107 (2009).
- [27] L. S. Brown and G. Gabrielse, *Rev. Mod. Phys.* **58**, 233 (1986).
- [28] K. Blaum, *Phys. Rep.* **425**, 1 (2006).
- [29] G. Gräff, H. Kalinowsky, and J. Traut, *Z. Phys. A* **297**, 35 (1980).
- [30] M. König, G. Bollen, H.-J. Kluge, T. Otto, and J. Szepo, *Int. J. Mass Spectrom.* **142**, 95 (1995).
- [31] G. Bollen, H.-J. Kluge, T. Otto, G. Savard, and H. Stolzenberg, *Nucl. Instrum. Meth. B* **70**, 490 (1992).
- [32] S. George, K. Blaum, F. Herfurth, A. Herlert, M. Kretzschmar, S. Nagy, S. Schwarz, L. Schweikhard, and C. Yazidjian, *Int. J. Mass Spectrom.* **264**, 110 (2007).
- [33] M. Kretzschmar, *Int. J. Mass Spectrom.* **264**, 122 (2007).
- [34] R. S. Van Dyck, F. L. Moore, D. L. Farnham, and P. B. Schwinberg, *Phys. Rev. A* **40**, 6308 (1989).
- [35] G. Bollen, H.-J. Kluge, M. König, T. Otto, G. Savard, H. Stolzenberg, R. B. Moore, G. Rouleau, G. Audi, and I. Collaboration, *Phys. Rev. C* **46**, R2140 (1992).
- [36] Kellerbauer, A., Blaum, K., Bollen, G., Herfurth, F., Kluge, H.-J., Kuckein, M., Sauvan, E., Scheidenberger, C., and Schweikhard, L., *Eur. Phys. J. D* **22**, 53 (2003).
- [37] R. T. Birge, *Phys. Rev.* **40**, 207 (1932).
- [38] P. J. Linstrom and W. G. Mallard, Eds., *NIST Chemistry WebBook*, NIST Standard Reference Database Number 69, National Institute of Standards and Technology, Gaithersburg MD, 20899, <http://webbook.nist.gov>, (retrieved May 24, 2016).
- [39] P. J. Mohr, D. B. Newell, and B. N. Taylor, *Rev. Mod. Phys.* **88**, 035009 (2016).
- [40] C. Patrignani and P. D. Group, *Chinese Physics C* **40**, 100001 (2016).
- [41] A. A. Kwiatkowski, T. Brunner, J. D. Holt, A. Chaudhuri, U. Chowdhury, M. Eibach, J. Engel, A. T. Gallant, A. Grossheim, M. Horoi, A. Lennarz, T. D. Macdonald, M. R. Pearson, B. E. Schultz, M. C. Simon, R. A. Senkov, V. V. Simon, K. Zuber, and J. Dilling, *Phys. Rev. C* **89**, 045502 (2014).
- [42] F. Köhler, K. Blaum, M. Block, S. Chenmarev, S. Eliseev, D. Glazov, M. Goncharov, J. Hou, A. Kracke, D. Nesterenko, Y. N. Novikov, W. Quint, E. M. Ramirez, V. M. Shabaev, A. Volotka, and G. Werth, *Nature Communications* **7**, 10246 (2016).
- [43] J. Ruyl and P. Endt, *Nuclear Physics A* **407**, 60 (1983).
- [44] J. Ruyl, J. D. Haas, P. Endt, and L. Zybert, *Nuclear Physics A* **419**, 439 (1984).
- [45] S. Rainville, J. K. Thompson, E. G. Myers, J. M. Brown, M. S. Dewey, E. G. K. Jr., R. D. Deslattes, H. G. Börner, M. Jentschel, P. Mutti, and D. E. Pritchard, *Nature* **438**, 1097 (2005).
- [46] M. Redshaw, J. McDaniel, and E. G. Myers, *Phys. Rev. Lett.* **100**, 093002 (2008).
- [47] M. Redshaw, R. Bryce, P. Hawks, N. Gamage, C. Hunt, R. Kandegedara, I. Ratnayake, and L. Sharp, *Nuclear Instruments and Methods in Physics Research Section B: Beam Interactions with Materials and Atoms* **376**, 302 (2016), proceedings of the XVIIth International Conference on Electromagnetic Isotope Separators and Related Topics (EMIS2015), Grand Rapids, MI, U.S.A., 11-15 May 2015.
- [48] M. S. Dewey and E. G. K. Jr., *J. Res. Natl. Inst. Stand. Technol.* **105**, 11 (2000).
- [49] T. D. Macdonald, B. E. Schultz, J. C. Bale, A. Chaudhuri, U. Chowdhury, D. Frekers, A. T. Gallant, A. Grossheim, A. A. Kwiatkowski, A. Lennarz, M. C. Simon, V. V. Simon, and J. Dilling, *Phys. Rev. C* **89**, 044318 (2014).



- [50] H. Schlermann and R. Böttger, Nuclear Physics A **501**, 86 (1989).
- [51] Maxime Mougeot, for the ISOLTRAP Collaboration, private communication.